# Chapter 2
# In Situ Modal Analysis of Gears

**F.M. Sciammarella, C.A. Sciammarella, and L. Lamberti**

**Abstract** There has been a vast amount of work in the analysis of multistage gearbox housings and the effects vibrations can have on them. This subject is of concern in the aerospace industry and is handled by Finite Element Analysis (FEA). Often experimental verification is required, particularly when a new design or material is introduced. Holographic interferometry and speckle interferometry are optical tools that provide in-situ comprehensive solutions when investigating the modal analysis of gears. Both of these experimental techniques provide an output that determines the dynamic characteristics of the gear being analyzed which can be directly connected to the FEA solution. Experimentally it is possible to obtain the dynamic displacement and strains for all the points of the area of interest and hence can be utilized to modify the FEA in such a way that the results of the FEA agree with experimental values. This type of analysis is particularly critical when it is important to determine the in-plane vibration modes of large gears, known as the "oval modes". These resonant modes are particularly important in aerospace applications because they can cause serious damage if left unchecked. The analysis of oval resonant modes were carried out on a spur gear to show the effectiveness and accuracy of this in-situ approach.

**Keywords** Gear resonance • Modal analysis • Image correlation • Vibration modes • Noise reduction

## 2.1 Introduction

The ability to reduce/eliminate noise and vibrations is of paramount importance for the aerospace industry. However, in order to make such reductions/eliminations, it is necessary to understand the reasons these vibrations occur. The aerospace industry has performed extensive analytical research into gear transmissions, in particular the effects which noise and vibration can have on the gear stages and the housing itself. In [1], by utilizing FEA, an analytical approach to understand the effects of a gearbox coupled vibration in a gear transmission system was developed and created another level of understanding in this field. The investigation presented in this paper deals with experimentally measuring and understanding resonant vibration modes of gears so that they can be utilized for FEA refinement. Resonant vibrations in mechanical structures occur when a natural frequency is at or close to a forcing frequency such as rotor speed. If generated during operation, this condition can cause severe vibration levels by amplifying small vibratory forces during operation. This type of condition can cause fatigue of gear teeth when they normally would not see such conditions. With this experimental approach it is possible to help confirm if in fact resonant modes will be generated based on FEA data provided of the systems response spectrum as a function of its oscillation regime.

This information is generated through FEA and is typically called a Campbell diagram (see Fig. 2.1).

F.M. Sciammarella (✉)
Department of Mechanical Engineering, College of Engineering & Engineering Technology, Northern Illinois University, 590 Garden Road, 60115 DeKalb, IL, USA
e-mail: sciammarella@niu.edu

C.A. Sciammarella
Department of Mechanical Engineering, College of Engineering & Engineering Technology, Northern Illinois University, 590 Garden Road, 60115 DeKalb, IL, USA

Department of Mechanical, Materials and Aerospace Engineering, Illinois Institute of Technology, 10 SW 32nd Street, 60616 Chicago, IL, USA
e-mail: sciammarella@iit.edu

L. Lamberti
Dipartimento Meccanica, Matematica e Management, Politecnico di Bari, Viale Japigia 182, 70126 Bari, Italy
e-mail: luciano.lamberti@poliba.it



H. Jin et al. (eds.), *Advancement of Optical Methods in Experimental Mechanics, Volume 3*, Conference Proceedings of the Society for Experimental Mechanics Series, DOI 10.1007/978-3-319-22446-6_2

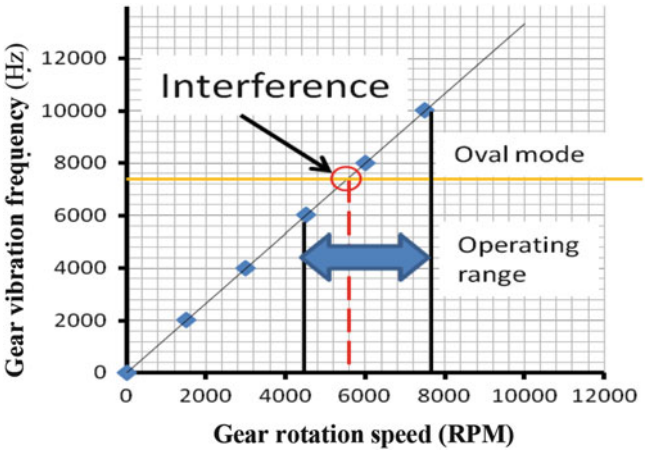


**Fig. 2.1** Campbell diagram of an aerospace gear indicating the RPM of the gear that produce interference with an oval mode (resonance) of the gear

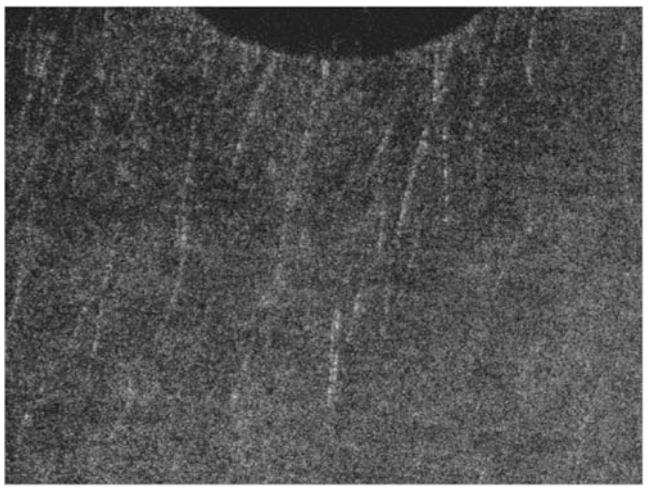

**Fig. 2.2** Fatigue micro-cracks at the root of a gear tooth caused by oval mode vibrations

Within the operating range of the gear the Campbell diagram shows that there is a resonance corresponding to an oval mode. This in-plane resonance of the gear produces displacements of magnitudes that conflict with the mechanical tolerances of the working gear. The consequences of this interference can be seen in Fig. 2.2.

As such, if a gear must be redesigned to remove these resonances it may result in increasing the gears weight, and considering the large accelerations that gears in aerospace applications are subjected to, the additional weight will create problems to the housing supporting the gear system. That is why it is critical to obtain experimental data to determine first the exact frequency at which this resonance occurs and the locations where it is highest. If the threshold displacements are low then perhaps a redesign may not be required.

There is one practical issue that must be dealt with when performing the experimental tests of these resonant oval modes, the high in-plane rigidity of a gear as compared with the rigidity of out-of-plane displacements. This problem is particularly acute in the case of large gears. In spite of the high sensitivity of techniques such as holography and speckle interferometry, the actual displacements that can be accurately measured are very small for allowable amounts of force that can be applied to excite a gear to vibrate in its resonant oval modes.

In order to solve the above described problem, a speckle interferometry method with the capability to determine dynamic displacements with nanometric accuracies was developed. This technique has been successfully applied to large heavy aerospace gears. The technique does not only determine with high accuracy the actual resonant frequencies but also the margin of frequencies around resonance that can still produce undesirable effects. These undesirable effects can hamper the gear from functioning properly.

## 2.2 Method to Determine the Gears Oval Resonant Modes

One issue that needs to be dealt with when utilizing holographic interferometry or speckle methods to get oval resonant modes of gears is generating enough energy to excite the structure. Classical methods to excite oval resonant-modes are: (1) supporting the gear on a shaker table; (2) or using a stinger. Both methods become difficult to implement when dealing

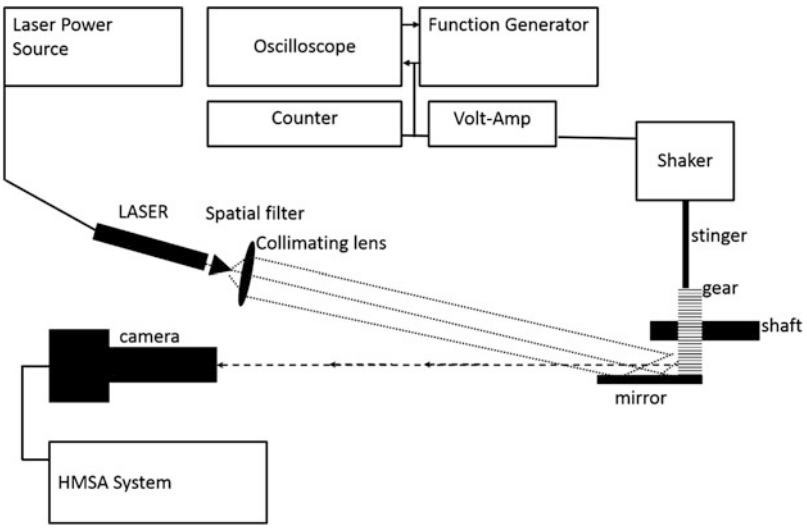


**Fig. 2.3** Optical set up to detect eigen-modes in large size gears

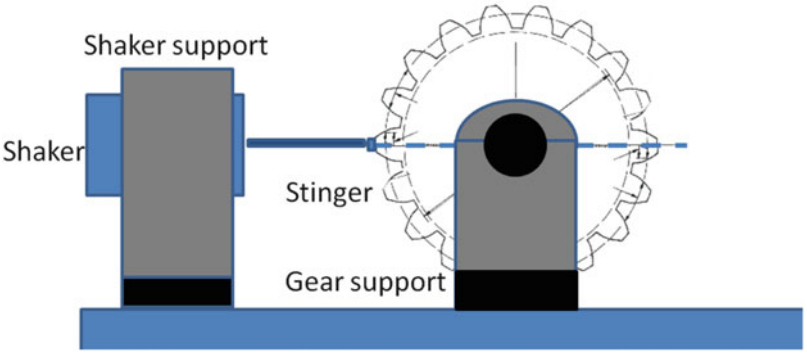


**Fig. 2.4** Shaker, stinger and gear

with large heavy gears. The shaker table requires a special installation which can be expensive. The stinger method will need a powerful high frequency piezoelectric shaker which can also be expensive. Another issue that could occur with using a stinger is that it could introduce problems with the fatigue life of the gear.

For all the above mentioned reasons an alternative solution was sought. The alternative needed to satisfy basic conditions mostly dictated by economic reasons: (a) utilize the stinger excitation method; (b) utilize of the shelf commercial piezoelectric shakers; (c) have a high frequency resolution because it is of interest not only to get the resonant frequencies but also monitor the process of inception of the resonant frequency; (d) have a very high sensitivity in view of the factors limiting the amount of force that can be applied to the gear.

It would be ideal to observe the full gear, however to reduce the forces required and to speed up the experimental analysis process it was decided to make observations in a region where it is possible to detect very small displacements. Because of the inverse relationship between the field of view with detectable displacements the observation is limited to a very small field of view, hence requiring a microscope in the observation part of the optical system.

Figure 2.3 shows a schematic of the set up utilized to make the measurements. Figure 2.4 shows how the stinger was aligned to the gear to ensure proper excitation.

Figure 2.5a shows the observed region (a zoomed view is shown in Fig. 2.5b) and Fig. 2.5c an amplified change of shape of the gear in the oval mode produced by the resonance of the gear.

The observed region corresponds to the maximum strain present in the dedendum circle of the gear due to the strain concentration at the notch between two successive teeth. In the region of observation the trajectories of the lines of maximum stress (isostatics) are tangent to the root of the notch. To get the necessary sensitivity, the observation is limited to a region of $2400 \times 500$ $\mu$m, region outlined by the rectangle of Fig. 2.5a. The selected method to measure displacements is speckle interferometry. Due to the strict tolerances in the fatigue life of the gear, it is important to know the order of magnitude of the strains in the region of observation. In order to get the sensitivity vector in the plane of observation, double illumination is utilized by means of collimated illumination and a mirror that creates the second wavefront as shown in Fig. 2.3. A solid state laser of wavelength $\lambda = 0.635$ $\mu$m is the source of illumination. The viewing system consists of a CCD camera with a microscope as the imaging system. The excitation is produced by a piezoelectric shaker that makes contact with the gear as shown in Fig. 2.4 through a stinger. The shaker is fed by a function generator through a voltage amplifier and a highly accurate

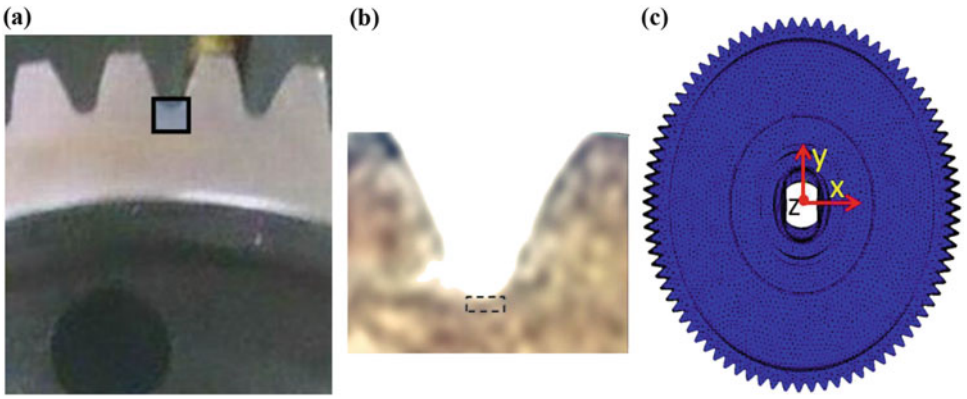


**Fig. 2.5** (**a**) Region of observation on the physical gear (actual size 2400 × 500 μm); (**b**) Zoomed view of the region of observation; (**c**) Oval mode with amplified changes of dimensions to visualize the changes experienced by the gear

counter measures the frequency of the sinusoidal excitation. An oscilloscope is utilized to perform calibration parameters of the input excitation. The shaker support and the support of the gear are rigidly connected to an optical table minimizing rigid body displacements.

## 2.3 Optical Method Utilized to Get the Strains in the Region of Interest

The optical setup is a classical double beam interferometer [2] with sensitivity given by,

$$\Delta u = \frac{\lambda}{2 \sin \theta} \tag{2.1}$$

where λ is the wavelength of the illuminating laser and θ is the angle made by the normal of the illumination plane wavefront with the normal of the observed surface.

The classical procedure to get the displacement information from speckle patterns is to display the correlation pattern between the reference or unloaded pattern and the deformed or loaded pattern. The correlation results in the display of fringes that upon filtering in the power spectrum of the Fourier transform (FT) yield the displacement information. The above described procedure works if the displacement u(x) is smaller than the radius of the speckle. If the displacement is larger than the speckle radius then correlation is lost. There are two causes that can make the displacement larger than the correlation radius: (1) the applied deformation exceeds the radius of correlation; (2) large rigid body motions generated by the applied loading.

For this study the small area under observation experienced rigid body motions as the gear was excited by the stinger. The excitation force applied by the stinger was practically constant for a given run and the rigid body motions of the observed region will get a steady state value. The actual displacements caused by the resonance phenomenon show an increasing periodic change of amplitude as the frequency approaches the resonance condition until a maximum displacement change is achieved. This maximum displacement change provides the resonance frequency. A further increase of the frequency causes the displacements to return to the values previous to the resonance.

In order to keep the correlation of the speckle patterns during the described process, the method utilized in [3–6] is applied. In [3, 4], it is shown that by digitally shifting two speckle patterns one with respect to the other a system of fringes appear in the Fourier space, a digital version of [7]. It is also shown that filtering at the first minimum of the fringes in the frequency space one obtains in the physical space a system of carrier fringes that contain the displacement information thus overcoming the decorrelation of speckles. This method was successfully applied to solve a number of problems described in [3–7] including very large deformations, $6 \times 10^4$ $\mu\varepsilon$, by step loadings. As shown in [3–5], the relative shifting of the final or loaded speckle pattern minus the initial speckle pattern produces a system of fringes in the physical space that after squaring the difference of the two patterns to get good visibility fringes are of the form,

$$S_s^2(x) = I \ [1 - \cos \phi(x)] \tag{2.2}$$

where the term $S_s^2(x)$ represents the signal produced by squaring of the difference of the two patterns, the letter I represents the intensity of the signal and the argument ϕ(x) contains the displacement information. The argument ϕ(x) is of the form,

$$\phi\,(\mathrm{x}) = [\Psi\,(\mathrm{x}) + \Delta\phi\mathrm{x}] \tag{2.3}$$

In Eq. (2.3), the term $\psi(x)$ represents the argument of the fringes produced by the rigid body displacement $\Delta_{Rx}$ and $\Delta\phi_x$ is the argument that provides displacement information generated by the deformations produced by the near resonance and resonance frequencies of the gear as the frequency of the applied force is changed with time.

As indicated in [3–5],

$$\psi(x) = \frac{2\pi}{\Delta_{Rx}}x \tag{2.4}$$

And

$$\Delta\phi_{\mathrm{x}} = 2\pi f_{\mathrm{p}} u\,(\mathrm{x}) \tag{2.5}$$

From Eq. (2.1)

$$f_p = \frac{2\sin\theta}{\lambda} \tag{2.6}$$

where $f_p$ is the spatial frequency of the double illumination fringes.

Then,

$$\Delta\phi_x\,(f_v) = \frac{4\pi\,\sin\theta}{\lambda}u\,(x, f_v) \tag{2.7}$$

where $f_v$ is the frequency of the exciting force in Hz. Finally, the equation of the fringes observed in the physical space is,

$$I(x) = I_o + I_1\,\cos 2\pi\left(\frac{x}{\Delta_{Rx}} + \frac{4\pi\,\sin\theta}{\lambda}u\,(x, f_v)\right) \tag{2.8}$$

This re-correlation technique was utilized on the limited region of the gear shown in Fig. 2.5a. Let us consider Fig. 2.6 where the segment $L_x$ represents the region under observation that experiences a rigid body translation $\Delta_{Rx}$ and an elongation due to deformation $\Delta_{Dx}$. The displacement due to deformation can be computed for this region,

$$\Delta_{Dx}\,(f_v) = \int_0^{L_x}\varepsilon_x\,(f_v, x)dx \tag{2.9}$$

Assuming the strain is a constant value $\varepsilon_{x0}(f_v)$ for the small segment and a given frequency then,

$$\Delta_{Dx}\,(f_v) = \varepsilon_{x0}\,(f_v)\,L_x \tag{2.10}$$

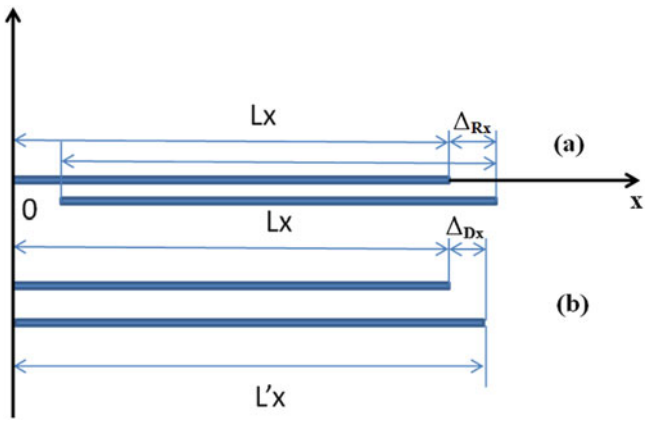


**Fig. 2.6** (**a**) Displacement of a segment $L_x$ due to rigid body motion along the coordinate axis x; (**b**) Deformation of the observed segment due to the strain caused by the resonance excitation

Finally, the total displacement of the observed region is given by,

$$\Delta_{Tx}(f_v) = \Delta_{Rx}(f_v) + \Delta_{Dx}(f_v) \tag{2.11}$$

In the FFT space for each stage of deformation one obtains a system of fringes whose spatial frequency will be a function of $\Delta_{Tx}(f_v)$. Since, as mentioned before, $\Delta_{Rx}$ in the steady state of vibration is a constant by measuring for each frequency one gets,

$$\varepsilon_{xo}(f) = \frac{\Delta_{Tx}(f) - \Delta_{Rx}}{L_x} \tag{2.12}$$

The preceding derivations assume a displacement in the X-direction but it is important to account for a rigid body rotation of the region under observation. The FT is rotation invariant hence a rotation in the physical space will rotate the spectra of the same amount, and then the speckle fringes in the FT space will be rotated by the same angle. Since we are dealing with projected displacements the fringe spacing in the FT must be corrected by the rotation effect.

To this point the derivations have not included the fact that the observed patterns are dynamic. The information being captured on the sensor is a harmonic function caused by an oscillatory motion given by the function $\cos(\omega t) = \cos(2\pi f_v t)$ that provides the frequency of the applied force. The observed pattern will be a time average pattern, that is it will be a pattern similar to the static pattern averaged in time,

$$< I(x,t) >= \frac{1}{T_{os}} \int_0^{T_{os}} I_o(t)\, dt + \int_0^{T_{os}} \frac{I_1(t)}{T_{os}} \cos 2\pi \left[ \left( \frac{2\sin\theta}{\lambda} \Delta_{Tx}\left(f_v\right) \right) \cos 2\pi f_v t \right] dt \tag{2.13}$$

where $T_{os}$ is the recording time of the observation camera. The resultant effect is described by the final equation,

$$\widetilde{I} = \widetilde{I_o} + \widetilde{I_1} \cos\left[(\phi_v)\right] \left\| J_0(\phi_v) \right\| \tag{2.14}$$

where,

$$\phi_v(f_v) = \frac{4\pi}{\lambda} \Delta_{Tx}(f_v) \tag{2.15}$$

The symbol "$\sim$" indicates the time average, and $||J_o(\phi_v)||$ is the absolute value of the zero-th order of the Bessel function of the argument $\phi_v(f_v)$. Equation (2.12) shows that the time averaged patterns in the frequency space are the resultant patterns of the squared subtraction of the two recorded speckle patterns but the amplitude of the resultant fringes is modulated by the absolute value of the zero-th order Bessel function of the argument $\phi_v(f_v)$.

Figure 2.7 shows the static fringes observed in the case of shifted speckle patterns [3] and the amount of shift in the frequency space obtained by applying the FT to the observed fringes. Figure 2.7c shows the dynamic fringes observed at the given frequency of 7500 Hz. These fringes show the translation and the rotation of the region of observation shown in Fig. 2.5a.

## 2.4 Procedure to Carry on the Measurements

In the standard method to get vibration modes of vibrating components utilizing moiré or speckle interferometry one sweeps a range of frequencies and visually detects the steady state fringes produced by the resonant modes. In general, only the value of the resonant frequency and node configurations are of interest and strain and stress values are actually obtained from dynamic finite element analyses. In the past, in complex problems where the application of finite elements is difficult or impossible to apply dynamic holographic interferometry was used to get quantitative data [8, 9]. In the present case at the outset quantitative data were of interest because of the requirement of detecting the onset of resonance and the range of frequencies around of the resonant mode. Furthermore, because of safety requirements of the inspected part, it was necessary to have a measure of the deformation applied to the part during testing for evaluation of the fatigue life of the part.

For the selected method of measurement it is not possible to utilize a direct visual observation of the resonance: hence, an alternative procedure was adopted. It was noticed that during the excitation of the gear assembly a distinct acoustic signal was emitted indicating the resonance of the gear.

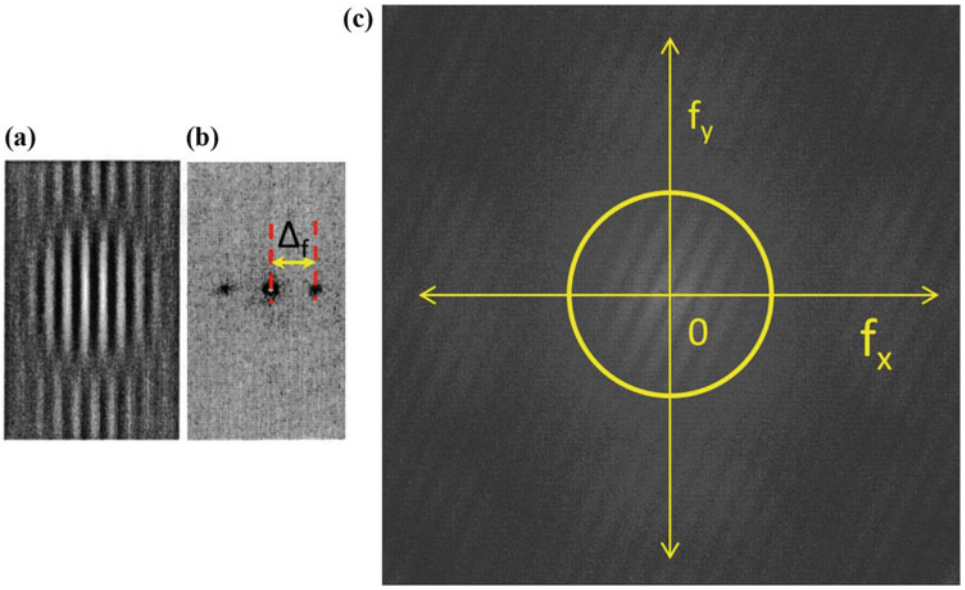


**Fig. 2.7** (**a**) Correlation fringe pattern in the FT space (static); (**b**) FT of the fringes shown in (**a**) and magnitude of the applied shift in the frequency space inverse of the shift in the physical space; (**c**) Correlation fringe pattern in the FT space (dynamic), 7500 Hz

**Table 2.1** Details of the observation system

| Camera | Infinity 3.1 megapixels |
|---|---|
| Image sensor | ½″ format, color, 6.5 × 4.9 mm |
| Effective pixels | 2048 × 1536, 3.2 μm square |
| Frame rate | 12 fps at 2048 × 1536 |
| Dynamic range | >60 db |
| Microscope | Infinity photo-optical |
| Field of view | 2400 μm |
| Magnification | 2.7 |
| NA | 0.0588 |
| Distance object-lens | 85 mm |
| Speckle size (measured) | 6 ± 0.9 μm |

## 2.5 Basic Properties and Parameters of the Illumination and the Observation System

The displacement resolution, a key parameter of the utilized method, depends on the illumination and observation system. The illumination system consists of a solid state laser with wavelength $\lambda = 0.635$ μm and 50 mW power. The angle of illumination is $\theta = 15°$ giving a sensitivity,

$$\Delta u = \frac{\lambda}{2 \sin \theta} \frac{1}{n} = 1.23 \ \ \mu\text{m/order} \tag{2.16}$$

A grating of pitch 100 μm was utilized to calibrate the image dimensions of 2048 × 1536 pixels resulting in the following quantities: $\Delta x = \Delta y = 1.171$ μm. Table 2.1 provides the different parameters of the observation system.

## 2.6 Data Gathering and Data Processing Procedures

As presented in Sect. 2.3, a shift between the initial or reference image and the subsequent images creates a carrier. In this particular case, the carrier was produced by the displacement introduced by the rigid body motion of the region under observation. At selected frequencies, dynamic images were recorded such as that shown in Fig. 2.7c.

The position of the first minimum after the coordinate's center was recorded for each dynamic image by performing five measurements for each image; values with a maximum $Std = \pm 1.28$ % were obtained. These values are plotted in the graph of Fig. 2.8. The oval mode of the analyzed gear region that is shown in Fig. 2.5c increases the radius of curvature of

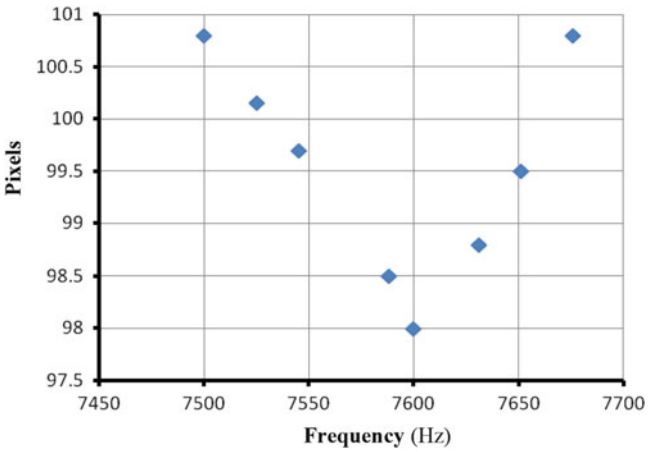


**Fig. 2.8** Pixel values for the first minimum at the recorded frequencies. Maximum value of the plot recorded at the frequency that produces the audible resonance

the dedendum gear circle (a small region of this circle is observed, Fig. 2.5a, b): hence, the region is subjected to tension. A tension decreases the frequency of the carrier fringes in the physical space since the pitch is increased (stretching). This means that the resultant pitch in the physical space is larger. The consequence in the frequency space is inverse, the number of pixels that represent the order or number of cycles in the physical space is reduced as shown in Fig. 2.8.

The number of cycles in the frequency space is obtained recalling that in the frequency space there are 1024 pixels or what is equivalent 1024 cycles. In the case of Fig. 2.7c the number of pixels for the first minimum is 100.80 then the corresponding N = 1024/100.8 = 10.1587 cycles where N is the order of the fringes. By applying the Nyquist condition that one cycle in the physical space is twice the value of one pixel, and calling this quantity $\delta_p$,

$$\delta_p = 2 \times 1.1718 \ \mu m/cycle \tag{2.17}$$

This quantity corresponds to the rigid body displacement of the observed region:

$$\Delta_{Rx}(f_v) = 2.3436 \ {}^{\mu m}\!/_{cycle} \times 10.1587 \ cycles = 23.808 \ \mu m \tag{2.18}$$

The resonance number of pixels is 98 pixels at $f_v = 7600$ Hz and the corresponding N is 1024/98 = 10.449 cycles/pixel. Then,

$$\Delta_{Tx}(f) = 2.3436 \ {}^{\mu m}\!/_{cycle} \times 10.449 pixel/cycle = 24.488 \ \mu m \tag{2.19}$$

Because the relationship between fringes spacing and displacements, the reduction of pitch implies an extension, from Eq. (2.9),

$$\Delta_{Dx}(f_v) = \Delta_{Tx}\left(f_v\right) - \Delta_{Rx}(f_v) \tag{2.20}$$

Then,

$$\Delta_{Dx}(f_v) = 24.488 - 23.808 = 0.680 \ \mu m \tag{2.21}$$

Since the sensitivity of the system to the in-plane displacement is 1.23 μm/order, the ratio of the displacement due to deformation to the in-plane sensitivity is,

$$r = \frac{0.680}{1.23} = 0.5528 \tag{2.22}$$

The above fraction of one order is easily detectable. The maximum strain at resonance is computed with Eq. (2.10),

$$\varepsilon_{xo}(f) = \frac{0.680 \ \mu m}{2400 \ \mu m} = 283 \times 10^{-6} \tag{2.23}$$

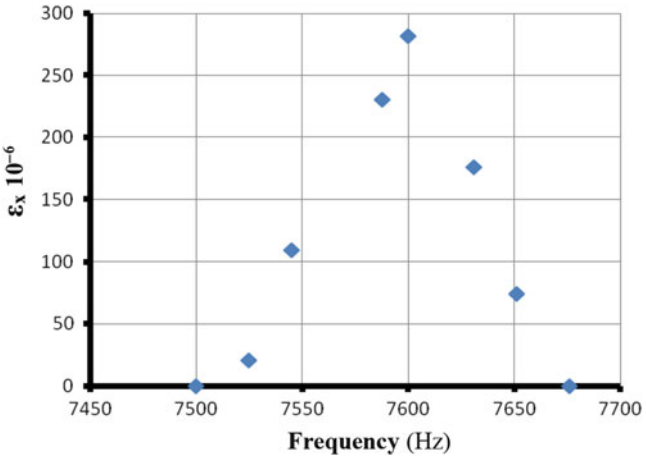


**Fig. 2.9** Microstrains as a function of the frequency in Hz

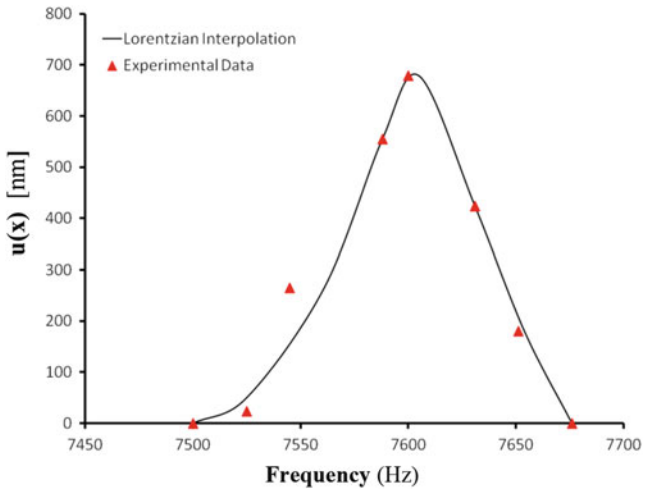


**Fig. 2.10** Displacements u(x) vs. frequency

Figure 2.9 shows the strains of the region under observation produced by the resonance of the gear as the frequency of the applied force is increased. Looking at the Campbell diagram represented in Fig. 2.1 one can understand the importance of knowing the extent of the frequencies where the resonance is taking place within the operating region of a gear.

The results shown in Fig. 2.9 correspond to a preliminary test program with a version of the gear preceding the final design. According to the computation using ANSYS, modal analysis gives, for the same oval mode reported in this paper, a resonance frequency of 7877 Hz. The difference between the experimental result for the oval mode frequency and the FE result for the subsequent iteration of the gear design is −3.51 %.

## 2.7 Discussion and Conclusions

The model introduced in [3–5] was successfully applied to a number of static problems with different materials. The research work presented in this paper is the first dynamic application of the method. The interpretation of the data requires analysis because in Eq. (2.12) the amplitude term is modulated by the Bessel function of the first kind and order zero. It is important to realize that the effect of the shift produce carrier fringes. If the magnitude of the rigid body motion remains a steady quantity, the spatial frequency of these fringes remains unchanged. The dynamic recording will reduce the visibility of the fringes as it can be observed in Fig. 2.7, when comparing the static shift fringes with the dynamic shift fringes. The part of the argument that is of interest is the displacement produced by the deformation of the gear tooth.

Figure 2.10 shows the displacements due to the applied deformation as a function of the frequency of the applied load. In the spatial coordinates the maximum displacement corresponds to an argument computed with Eq. (2.13). That is:

$$\phi_v\left(f_v\right) = \frac{4\pi}{\lambda}\Delta D_x\left(f_v\right) = \frac{4\pi}{0.635}0.680 = 13.450 \tag{2.24}$$

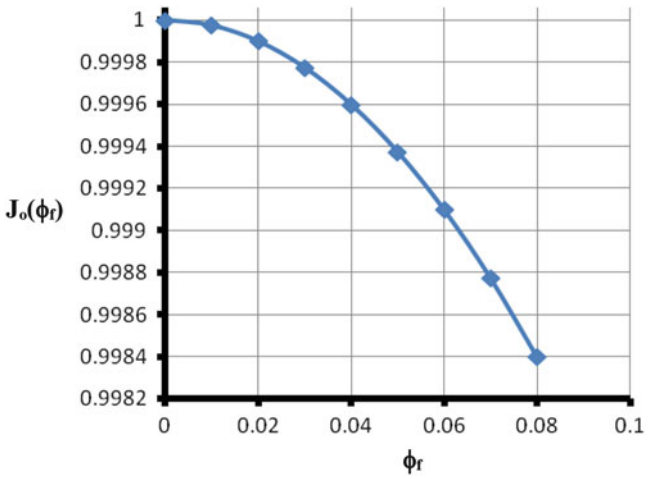


**Fig. 2.11** Variation of the function $J_o(\phi_f)$ for the frequency space changes caused by the displacements due to the observed deformations

In the frequency space, the argument is the inverse quantity,

$$\phi_f = 0.0744 \tag{2.25}$$

As shown by Fig. 2.11 the effect of the amplitude modulation caused by frequency changes due to the displacements produced deformations are negligible in the frequency space. It is interesting to note, Fig. 2.10, that the resonant points have an asymmetric Lorentzian type of distribution which is observed in the resonance phenomenon of many different physical systems with harmonic excitation and damping. This type of distribution is detected in forced harmonic vibrations of steel structures.

In conclusion, it is possible to say that the method of creating carrier fringes in speckle interferoemtry by shifting patterns has been extended to periodic dynamic measurements. This extension is a powerful in situ tool to measure displacements in the nanometric range thus opening the possibility of extending the capabilities of time average dynamic speckle interferometry to analyze resonant modes that are difficult to excite in view of the involved structural rigidity as is the case of the gear analyzed in the present paper.

## References

1. F.K. Choy, Y.F. Ruan, R.K. Tu, J.J. Zakrajsek, D.P. Townsend, Modal analysis of multistage gear systems coupled with gearbox vibrations. J. Mech. Des. **114**(3), 486–497 (1992)
2. C.A. Sciammarella, F.M. Sciammarella, *Experimental Mechanics of Solids*. (Wiley, Chichester, Chapter 18, 2012), pp. 573−576
3. C.A. Sciammarella, F.M. Sciammarella (1998) On the nature of the optical information recorded in speckles, in *Proceedings of the International Conference on Applied Optical Metrology*, Hungary, June 1998. *Proceedings of the SPIE* 3407:8–11
4. C.A. Sciammarella, F.M. Sciammarella, Extension of the electronic speckle correlation interferometry to large deformations, in *Laser interferometry IX, Applications*, ed. by R.J. Pryputniewicz, G.M. Brown, W.P.O. Jueptner, *Proceedings of SPIE 3479*, 1998, pp. 252–263
5. C.A. Sciammarella, F.M. Sciammarella, An extension of holographic moiré to micromechanics, in *Proceeding of the IUTAM Symposium on Advances in Optical Methods for Applied Solid Mechanics*, ed. by A. Lagarde (Kluwer Academic, The Netherlands, 2000), pp. 451–466
6. C.A. Sciammarella, F.M. Sciammarella, Measurement of mechanical properties of materials in the micrometric range using electronic holographic moiré. Opt. Eng. **42**(5), 1215–1222 (2003)
7. J.M. Burch, M.J. Tokarski, Production of multiple beam fringes from photographic scatters. Opt. Acta **17**(2), 101–111 (1968)
8. C.A. Sciammarella, M. Ahmadshahi, Non-destructive evaluation of turbine blades vibrating in resonant modes. In: *Moiré Techniques, Holographic Interferometry, Optical NDT and Application to Fluid Mechanics*, ed. by F.P. Chiang, *Procedings of SPIE* 1554B, 1991, pp 743–753
9. C.A. Sciammarella, C. Casavola, L. Lamberti, C. Pappalettere, Fracture of turbine blades under self-exciting modes. Strain **47**, 113–129 (2011)

http://www.springer.com/978-3-319-22445-9

Advancement of Optical Methods in Experimental Mechanics, Volume 3
Proceedings of the 2015 Annual Conference on Experimental and Applied Mechanics
Jin, H.; Yoshida, S.; Lamberti, L.; Lin, M.-T. (Eds.)
2016, IX, 316 p., Hardcover
ISBN: 978-3-319-22445-9